Morgan, D. O., & Roth, R. A. (1987) *Proc. Natl. Acad. Sci. U.S.A. 84*, 41-45.
Morrison, B. D., & Pessin, J. E. (1987) *J. Biol. Chem. 262*, 2861-2868.
Neil, J. C., Ghysdael, J., Vogt, P. K., & Smart, J. (1981) *Nature 291*, 675-677.
Patchinsky, T., & Sefton, B. (1981) *J. Virol. 39*, 104-114.
Patchinsky, T., Hunter, T., Esch, F. S., Cooper, J. A., & Sefton, B. M. (1982) *Proc. Natl. Acad. Sci. U.S.A. 79*, 973-977.
Pearson, R. B., Wettenhall, R. E. H., Means, A. R., Hartshome, D. J., & Kemp, B. E. (1988) *Science 241*, 970-973.
Rees-Jones, R. W., & Taylor, S. C. (1985) *J. Biol. Chem. 260*, 4461-4467.
Rosen, O. M., Herrera, R., Olowe, Y., Petruzzelli, L. M., & Cobb, M. H. (1983) *Proc. Natl. Acad. Sci. U.S.A. 80*, 3237-3240.
Ross, E. M., & Gilman, A. G. (1980) *Annu. Rev. Biochem. 49*, 533-564.
Sahal, D., Ramachandran, J., & Fujita-Yamaguchi, Y. (1988) *Arch. Biochem. Biophys. 260*, 416-426.
Schramm, M., & Selinger, Z. (1984) *Science 225*, 1350-1356.
Scoffone, E., Fontana, A., & Rocchi, R. (1968) *Biochemistry 7*, 971-979.
Shechter, Y., Burstein, Y., & Patchornik, A. (1972) *Biochemistry 11*, 653-660.
Shechter, Y., Burstein, Y., & Patchornik, A. (1975) *Biochemistry 14*, 4497-4503.
Smart, J. E. (1981) *Proc. Natl. Acad. Sci. U.S.A. 78*, 6013-6017.
Stadtmaver, L. A., & Rosen, O. M. (1983) *J. Biol. Chem. 258*, 6682-6685.
Toi, K. E., Bynum, E., Norris, E., & Itano, H. A. (1967) *J. Biol. Chem. 242*, 1036-1043.
Walker, D. H., Kupuswamy, D., Visvanathan, A., & Pike, L. J. (1987) *Biochemistry 26*, 1428-1433.
White, M. F., Maron, R., & Kahn, C. R. (1985) *Nature 318*, 183-186.
White, M. F., Stegman, E. W., Dull, T. J., Ullrich, A., & Kahn, C. R. (1987) *J. Biol. Chem. 262*, 9769-9777.
Wong, T. W., & Goldberg, A. R. (1983) *J. Biol. Chem. 261*, 10000-10005.
Yu, K. T., & Czech, M. P. (1984) *J. Biol. Chem. 259*, 5277-5286.

Yeast Allosteric Chorismate Mutase Is Locked in the Activated State by a Single Amino Acid Substitution†

Tobias Schmidheini,‡ Hans-Ulrich Mösch,‡ Jeremy N. S. Evans,§ and Gerhard Braus*,‡

Institut für Mikrobiologie, Eidgenössische Technische Hochschule, Schmelzbergstrasse 7, CH-8092 Zürich, Switzerland, and Biochemistry-Biophysics Program, Washington State University, Pullman, Washington 99164-4660

Received September 5, 1989; Revised Manuscript Received December 5, 1989

ABSTRACT: Chorismate mutase, a branch-point enzyme in the aromatic amino acid pathway of *Saccharomyces cerevisiae*, and also a mutant chorismate mutase with a single amino acid substitution in the C-terminal part of the protein have been purified approximately 20-fold and 64-fold from overproducing strains, respectively. The wild-type enzyme is activated by tryptophan and subject to feedback inhibition by tyrosine, whereas the mutant enzyme does not respond to activation by tryptophan nor inhibition by tyrosine. Both enzymes are dimers consisting of two identical subunits of M_r 30000, each one capable of binding one substrate and one activator molecule. Each subunit of the wild-type enzyme also binds one inhibitor molecule, whereas the mutant enzyme lost this ability. The enzyme reaction was observed by ^{1}H NMR and shows a direct and irreversible conversion of chorismate to prephenate without the accumulation of any enzyme-free intermediates. The kinetic data of the wild-type chorismate mutase show positive cooperativity toward the substrate with a Hill coefficient of 1.71 and a $[S]_{0.5}$ value of 4.0 mM. In the presence of the activator tryptophan, the cooperativity is lost. The enzyme has an $[S]_{0.5}$ value of 1.2 mM in the presence of 10 μM tryptophan and an increased $[S]_{0.5}$ value of 8.6 mM in the presence of 300 μM tyrosine. In the mutant enzyme, a loss of the cooperativity was observed, and $[S]_{0.5}$ was reduced to 1.0 mM. This enzyme is therefore locked in the activated state by a single amino acid substitution.

The binding of an effector at an allosteric site of an enzyme with the induction of a conformational change appears to form the basis for many aspects of regulation. Most allosteric enzymes are oligomeric, and binding of allosteric effectors leads to an altered conformational state having a different binding constant for effectors. One model describing this conformational change was proposed by Monod et al. (1965). According to this model, an allosteric enzyme consists of an equilibrium of a T (tense) state, having a lower substrate affinity, and an R (relaxed) state, having a higher substrate affinity. Increasing substrate concentrations pull the T-R equilibrium toward the R state with a higher substrate affinity, which results in a sigmoidal substrate saturation curve (positive cooperativity). An activator, however, transforms the equilibrium toward the R state, resulting in an equal binding

† Supported by Swiss National Foundation Grant 3.654-0.87.
* Address correspondence to this author.
‡ Eidgenössische Technische Hochschule.
§ Washington State University.

0006-2960/90/0429-3660$02.50/0

affinity for all substrate molecules. Thus, at saturating activator concentrations, the substrate binding obeys Michaelis–Menten kinetics. This effect, in which cooperativity is destroyed in the presence of an activator thus leading to a hyperbolic substrate saturation curve, has been observed for allosteric enzymes such as the isocitrate dehydrogenase of *Saccharomyces cerevisiae* (Hathaway & Atkinson, 1963) and the deoxythymidine kinase of *Escherichia coli* (Okazaki & Kornberg, 1964).

We investigated the allosteric *S. cerevisiae ARO7* gene product chorismate mutase, and in addition, we demonstrate the striking effect of a single amino acid exchange on the allosteric regulation. In *S. cerevisiae*, the anthranilate synthase complex and the *ARO7* gene product chorismate mutase control the distribution of chorismate at the first branch point of the aromatic amino acid biosynthetic pathway. The chorismate mutase is a monofunctional enzyme and catalyzes the conversion of chorismate to prephenate, leading to phenylalanine and tyrosine, whereas the anthranilate synthase complex is the first enzyme in the tryptophan pathway. The flux of chorismate is regulated by tryptophan which acts as a feedback inhibitor of anthranilate synthase and as activator of chorismate mutase (Prantl et al., 1985; Kradolfer et al., 1977). Tyrosine, however, is a feedback inhibitor of chorismate mutase (Kradolfer et al., 1977). Whereas all other aromatic amino acid biosynthetic genes are regulated by the transcriptional activator GCN4 (Paravicini et al., 1989a; Miozzari et al., 1978; Hinnebusch, 1988), the *ARO7* and the *TRP1* genes are not regulated at the transcriptional level (Schmidheini et al., 1989; Braus et al., 1988). The *ARO7* gene and also the three *ARO7*^{c} mutant alleles were isolated and sequenced previously (Schmidheini et al., 1989). The mutant alleles encode constitutively activated chorismate mutases as a result of an amino acid substitution, Thr226 to Ile226.

In this work, we purified both the wild-type and the mutant chorismate mutase and used the wild-type enzyme as a model for an allosteric enzyme. We investigated the native molecular weight of both enzymes and observed the enzyme reaction in a time course using ^{1}H NMR spectroscopy. Kinetic assays and binding studies on both enzymes were performed. The wild-type enzyme is regulated by an inhibitor and an activator whereas the mutant enzyme is frozen in the R state and cannot be regulated by altering the T–R equilibrium.

Materials and Methods

Materials. Chorismic acid (as barium salt) and phenylmethanesulfonyl fluoride (PMSF)[1] were purchased from Sigma (St. Louis, MO). Sepharose CL4B, MonoQ column (HR16/10), Sephadex G-75, Sephacryl S-300, and the FPLC system were from Pharmacia (Uppsala, Sweden). Ethylamino-Sepharose was synthesized by the method of Jenissen and Heilmeyer (1975) using Sepharose CL4B as matrix. For protein concentration and desalting, stirred cells and PM-10 ultrafiltration membranes from Amicon (Danvers, MA) were used. L-[*methylene*-^{14}C]Tryptophan (54 mCi/mmol) and L-[U-^{14}C]tyrosine (486 mCi/mmol) were obtained from Amersham (Amersham, U.K.). For equilibrium dialysis, polypropylene equilibrium dialysis cells having a volume of 0.2 mL for each compartment were used as described in Englund et al. (1969). All other chemicals were from either Fluka (Buchs, Switzerland), Merck (Darmstadt, FRG), or Sigma (St. Louis, MO).

Strains, Media, Plasmids, and Growth Conditions. All yeast strains used are derivatives of the *S. cerevisiae* laboratory strain X2180-1A (*MATa gal2 SUC2 mal CUP1*) and X2180-1B (*MATα gal2 SUC2 mal CUP1*). The RH1242 genotype is *MATα aro7 leu2-2*. Plasmids pME605 and pME606 containing the wild-type and the mutant *ARO7* gene, respectively, are derivatives of pJDB207 (Beggs, 1978) and were described previously (Schmidheini et al., 1989). For the purification of the wild-type chorismate mutase, strain RH1242 transformed with pME605, and for the mutant enzyme the same strain transformed with pME606, was used. Cells were grown on MV-minimal medium (Miozzari et al., 1978) at 30 °C in 5-L Erlenmeyer flasks with indentations on a rotary shaker and harvested in mid-log phase at a density of A_{546} = 4. For strain RH1242 (pME606), the minimal medium had to be supplemented with tryptophan (50 mg/L). For a typical purification procedure, 100 g of wet cell paste was used.

Enzyme Assay. Enzyme activities are specified in International Units (1 unit = the appearance of 1 μmol of product per minute). The chorismate mutase was measured with a stop assay (Schmidheini et al., 1989). No direct assay measuring the appearance or disappearance of substrate/product was possible because of excessive UV absorbance at high substrate concentrations. Therefore, for steady-state kinetics, the reaction time was reduced to 2 min, and the measurements were controlled for linearity during this time. For determination of the pH optima, a universal buffer solution with a pH range of 2.6–12.0 containing 30 mM citric acid, 30 mM KH_2PO_4, 30 mM H_3BO_3, 30 mM diethylbarbituric acid, and different concentrations of NaOH was used (Dawson et al., 1969).

The protein content was measured by the method of Lowry et al. (1951) for determination of the specific enzyme activity, or by the quick method of Bradford (1976) during the protein purification.

Purification of the Chorismate Mutase. Both the wild-type and the mutant chorismate were purified by the same procedure. Crude extracts from 80–120 g of wet cell paste were prepared as described previously (Kradolfer et al., 1977), omitting the desalting step on Sephadex G-25. DTT (1 mM), PMSF (0.1 mM), and EDTA (0.1 mM) were used for all purification steps. Routine preparations were carried out at 4 °C.

(*1*) *Ammonium Sulfate Precipitation.* The potassium phosphate concentration of the crude extract was increased to 0.5 M (pH 7.6) by adding the appropriate amount of K_2HPO_4. The solution was then adjusted to 40% saturation with ammonium sulfate, and the pH was corrected to 7.6 if necessary. After 20 min of stirring at 4 °C, the precipitate was removed by centrifugation at 25000*g* for 20 min, yielding ammonium sulfate extract.

(*2*) *Hydrophobic Interaction Chromatography.* The ammonium sulfate extract was loaded on an ethylamino-Sepharose column (2.6 × 40 cm) previously equilibrated with 0.5 M potassium phosphate buffer, pH 7.6, at 40% saturation with ammonium sulfate (containing no PMSF). The binding capacity of the material was 20 mg of protein/mL. After being washed with 2 column volumes of the same buffer, adsorbing proteins were eluted with a linear gradient of decreasing potassium phosphate and decreasing ammonium sulfate concentration from equilibration buffer to H_2O. Ten-milliliter fractions were collected at a flow rate of 1 mL/min. Fractions

[1] Abbreviations: DAHP, 3′-deoxy-D-arabinoheptulosonate 7-phosphate; DTT, dithiothreitol; EDTA, ethylenediaminetetraacetic acid; FPLC, fast protein liquid chromatography; PMSF, phenylmethanesulfonyl fluoride; SDS, sodium dodecyl sulfate.

containing chorismate mutase activity were pooled and desalted several times against 10 mM Tris-HCl, pH 7.6, using a stirred cell.

(*3*) *Anion-Exchange Chromatography.* An FPLC MonoQ column (HR 16/10) was equilibrated with 10 mM Tris-HCl, pH 7.6, and the concentrated ethylamino-Sepharose fractions were applied to the column, which was washed with 100 mL of the same buffer. The adsorbed proteins were eluted in a 300-mL linear gradient of NaCl (0–200 mM) in equilibration buffer using a flow rate of 4 mL/min. Peak fractions of 4 mL containing chorismate mutase activity were pooled and applied a second time on the same MonoQ column after desalting.

(*4*) *Gel Filtration on Sephadex G-75.* The second MonoQ pool was concentrated to 2 mL and applied on a Sephadex G-75 column (2.6 × 70 cm) previously equilibrated with 20 mM Tris-HCl, pH 7.6. The protein was eluted at a rate of 0.25 mL/min and collected as 2-mL fractions. Fractions containing pure chorismate mutase were pooled, concentrated, and stored in 50% glycerol containing 1 mM DTT.

Amino Acid Sequence Determination. The amino acid sequence of the chorismate mutase was analyzed by immobilizing tryptic polypeptides on glass fiber disks according to Aebersold et al. (1987) and using a gas-phase sequencer (Applied Biosystems Inc., Model 470A) directly linked to a phenylthiohydantoin analyzer.

Acid Hydrolysis and Amino Acid Analysis. The part of the glass fiber sheet containing the protein was cut out and subjected to acid hydrolysis and amino acid analysis as described previously (Aebersold et al., 1987) using a Waters Pico-Tag system.

Formate Cleavage. Purified chorismate mutase was cleaved at a concentration of 0.5 μg/μL in 70% formate at 37 °C (Landon, 1977). After 48- and 72-h incubation, the formate was evaporated, the samples were resuspended in 50 mM Tris-HCl, pH 7.6, and analyzed on a 15% SDS–polyacrylamide gel.

Determination of the Native Molecular Weight. The native molecular weight of the chorismate mutase was estimated by gel filtration on a Sephacryl S-300 column using 20 mM Tris-HCl, pH 7.6, 100 mM NaCl, and 1 mM DTT as the elution buffer and chymotrypsinogen, ovalbumin, bovine serum albumin, and blue dextran as calibration markers. In addition, the molecular weight was independently determined by sedimentation equilibrium at 14 000 rpm (12 °C), and the molecular mass was calculated by the linear least-squares fit of ln A_{280} versus r^2. The sedimentation velocity at 56 000 rpm (20 °C) was also determined. All ultracentrifugation analyses were performed on a Beckman Model E equipped with a photoelectric scanner system. The buffer was 50 mM potassium phosphate, pH 7.6, 0.1 M NaCl, and 1 mM DTT.

NMR Spectroscopy. High-field Fourier-transform (FT) NMR studies were performed on a Bruker AM-500 (11.75 T, 500 MHZ ^{1}H) NMR spectrometer. Deuterium was used for locking the field. Proton chemical shifts were referenced externally to sodium 3-(trimethylsilyl)propanoate-*2,2,3,3-d*$_4$ (TSP) in D_2O buffer (δ_H = 0.00 ppm). Water suppression in ^{1}H NMR spectra was achieved by homonuclear irradiation. Sample temperature was maintained with a Burker VT-100 variable-temperature control unit, using boil-off liquid nitrogen. All experiments reported here were carried out at 4 °C.

Equilibrium Dialysis. For tryptophan binding determination, a stock solution of 300 μM L-[*methylene*-^{14}C]tryptophan at a final radiochemical concentration of 9 μCi/mL in 50 mM potassium phosphate buffer, pH 7.6, was prepared. Different dilutions of this stock solution were added to one of the dialysis cell compartments, and a solution of 14.5 μM chorismate mutase was added to the other compartment. After 3-h equilibration at 30 °C, the tryptophan concentration on each side of the dialysis cell was determined by using scintillation counting. Free (A_f) and bound (A_b) tryptophan concentrations were calculated. The final protein concentration in each compartment was checked by enzyme assay. In all cases, no leakage of the membrane could be detected. The purity of the L-[*methylene*-^{14}C]tryptophan was checked by thin-layer chromatography on silica gel 60, using 1-butanol/acetic acid/water (12:3:5) for separation. Less than 5% impurities could be visualized after autoradiography. The same procedure was used for determining tyrosine binding using a stock solution of 1 mM L-[U-^{14}C]tyrosine at a final radiochemical concentration of 2 μCi/mL.

Results

Purification of the Wild-Type and Mutant Chorismate Mutase of S. cerevisiae. Both enzymes were purified from the *aro7 leu2* double-mutant strain RH1242 carrying the wild-type *ARO7* or the mutant *ARO7*^{c} gene cloned on the high copy number plasmid pJDB207 (Beggs, 1978). These plasmid-carrying strains overexpressed the wild-type enzyme more than 500-fold and the mutant enzyme more than 150-fold in comparison to a yeast strain with a single chromosomal copy. Therefore, overexpression serves as a first step in the purification procedure for both the wild-type and the mutant chorismate mutase. The specific activity of the chromosomally encoded chorismate mutase was measured at 1 mM chorismate as 1.5 milliunits/mg for the wild-type and 17 milliunits/mg for the mutant enzyme (Schmidheini et al., 1989). Surprisingly, strain RH1242 (pME606), overexpressing the mutant chorismate mutase, did not grow in minimal media, suggesting that the high activity of the mutant chorismate mutase, which channels chorismate directly into phenylalanine and tyrosine, causes a lack of tryptophan. Presumably, anthranilate synthase, which is the enzyme responsible for the first step in the tryptophan biosynthetic branch, is no longer able to compete with this high chorismate mutase activity. This problem was overcome by supplementation with tryptophan.

Both enzymes eluted in all columns at the same salt concentration. The ethylamino-Sepharose column released the enzyme at 250 mM potassium phosphate concentration, whereas for the MonoQ column, the chorismate mutase was eluted at 80 mM NaCl. The wild-type chorismate mutase was further purified by gel filtration on Sephadex G-75, whereas the mutant enzyme was pure after the second MonoQ column. The purification procedure is summarized in Figure 1. An SDS–polyacrylamide gel (Figure 1A,B) shows a strong band at M_r 29 000 for both enzymes, which corresponds to the molecular weight previously deduced from the DNA sequence (29 750; Schmidheini et al., 1989).

The wild-type enzyme was purified 21-fold with a 26% yield of recovery. Including the 520-fold overexpression due to the high copy number of the plasmid, this corresponds to an 11 000-fold enrichment of the chromosomally encoded wild-type chorismate mutase. The 64-fold purification and the 150-fold overexpression of the mutant enzyme give approximately the same enrichment factor. At a concentration of 1 mg/mL, both enzymes were stable for more than 6 months, in 100 mM Tris-HCl, pH 7.6 at 4 °C, as well as in 50% glycerol at −20 °C.

Analysis of the Amino Acid Sequence. No N-terminal amino acid sequence could be detected by Edman degradation of the wild-type chorismate mutase, indicating a blocked N-terminus.

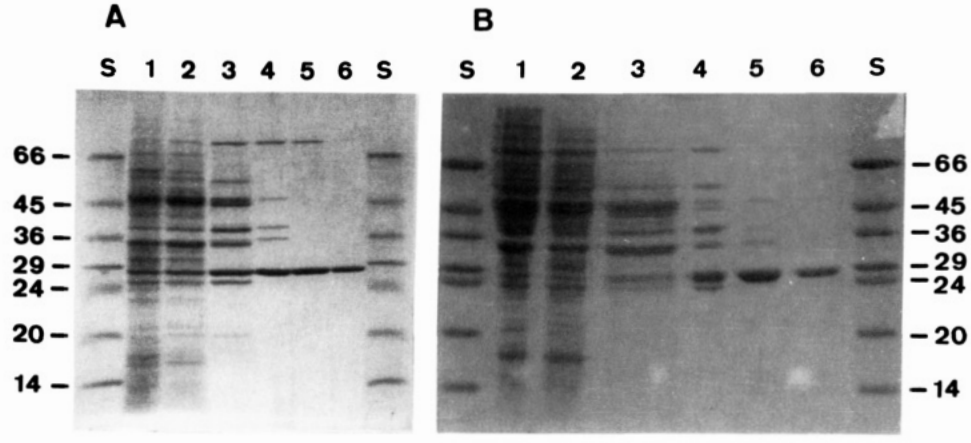

C

fraction	total protein (mg)	spec. activity (U/mg)	yield (%)	purification (x-fold)
crude extract	3230 (6970)	0.78 (3.1)	100 (100)	
ammonium sulfate	1925 (2700)	1.16 (7.5)	89 (94)	1.5 (2.4)
ethylamino Sepharose	298 (255)	5.35 (54.3)	64 (64)	6.9 (17.6)
first MonoQ	93 (67)	11.07 (189.8)	41 (59)	14.3 (61.5)
second MonoQ	60 (42)	12.73 (197.6)	31 (39)	16.4 (64.0)
Sephadex G-75	41	16.04	26	20.6

FIGURE 1: Purification steps of the wild-type and the mutant chorismate mutase of *S. cerevisiae*. (A) SDS–polyacrylamide gel of the purification steps of the wild-type enzyme. 1, Crude extract of RH1242 (pME605) (50 μg); 2, supernatant of ammonium sulfate precipitation (50 μg); 3, ethylamino-Sepharose pool (20 μg); 4, first MonoQ pool (15 μg); 5, second MonoQ pool (12 μg); 6, Sephadex G-75 pool (5 μg); S, marker proteins with the indicated molecular mass in kilodaltons for bovine albumin (66), egg albumin (45), glyceraldehyde-3-phosphate dehydrogenase (36), carbonic anhydrase (29), trypsinogen (24), trypsin inhibitor (20), and α-lactalbumin (14). (B) SDS–polyacrylamide gel of the purification steps of the mutant enzyme. 1, crude extract of the wild-type strain X2180-1A (40 μg); 2, crude extract of RH1242 (pME606) (40 μg); 3, supernatant of ammonium sulfate precipitation (15 μg); 4, ethylamino-Sepharose pool (10 μg); 5, first MonoQ pool (8 μg); 6, second MonoQ pool (4 μg). (C) Purification protocol for the yeast chorismate mutase. The values for the mutant chorismate mutase are given in parentheses; 1 mM chorismate was used as substrate for enzyme assays.

In order to verify the earlier determined DNA sequence, five tryptic fragments were sequenced (Figure 2A, underlined). The amino acid sequences of all fragments agreed with the predicted sequence.

From the DNA sequence, it is not clear whether the first or the second methionine is used as a translation start point (Figure 2A, positions 1 and 22). Therefore, the N-terminus of the wild-type chorismate mutase was determined indirectly; the protein was cleaved with formate between Asp215 and Pro216. The polypeptide ranging from Met22 to Asp215 has a theoretical molecular weight of 22 215, in contrast to 24 853 for the longer peptide Met1 to Asp215. The latter polypeptide can be detected on an SDS–polyacrylamide gel (Figure 2B), suggesting that the first methionine is used for translation initiation and forms the N-terminus of the native protein. These data were confirmed by a total acid hydrolysis of the pure wild-type chorismate mutase. The amino acid composition agrees with that deduced from the nucleotide sequence of the *ARO7* gene starting at the first methionine (Figure 2C).

Apparent Native Molecular Weight. The native molecular weight of both the wild-type as well as the mutant enzyme was determined by gel filtration and ultracentrifugation analysis. A molecular weight of 51 000 for the wild-type and 53 000 for the mutant chorismate mutase was estimated from a calibrated Sephacryl S-300 column, in the absence of the activator tryptophan as well as in its presence at a concentration of 0.5 mM (data not shown). The molecular mass obtained from sedimentation equilibrium was 61 000 ± 4000 for the wild-type and 64 000 ± 4000 for the mutant enzyme, respectively (data not shown). Taking into account the molecular weight of a single subunit of 29 750 as judged from the DNA sequence as well as from an SDS–polyacrylamide gel, the results of the gel filtration and of the ultracentrifugation suggest that the chorismate mutase has to be a dimer of two identical subunits. The sedimentation coefficient $s_{20,w}$ was 3.6 S for the wild-type and 3.8 S for the mutant enzyme.

NMR Studies. The enzymic course of the reaction catalyzed by purified chorismate mutase has been examined by ^{1}H NMR spectroscopy. Figure 3A shows the conversion of chorismate to prephenate over a time course of 180 min. Spectra were recorded at intervals of 4 min. Resonances due to chorismate (H2, 6.1 ppm; H6, 5.8 ppm; H5, 5.5 ppm; H9, 4.7 ppm; H3, 4.4 ppm; H4, 4.3 ppm; H9, 4.1 ppm) reduce in intensity with time, and resonances due to prephenate (H2,6, 5.55 ppm; H3,5 5.45 ppm; H4, 4.1 ppm; H8, 2.7 ppm) increase correspondingly. Apart from an impurity present at all times at 3.1 ppm, no additional resonances are detected throughout the course of reaction. This establishes that no side reactions occur and that no enzyme-free intermediates accumulate. Figure 3B shows the ^{1}H NMR spectrum of chorismate mutase itself (at 2 mM). This suggests that the protein is largely aggregated, at a minimum as a dimer (on the basis of the ^{1}H line widths). The dimer to monomer dissociation cannot be affected by altering the concentration (0.5–2 mM), the ionic strength (in 0–1 M KCl), or the hydrophobicity (in 0–60% methanol-d_4) (data not shown). Progressive additions of the chaotropic agent guanidine hydrochloride (0–6 M) to chorismate mutase resulted in very little change in the spectra until around 4 M guanidine hydrochloride, at which point complete unfolding occurs. This suggests that dissociation of the dimeric structure only occurs with unfolding of the monomers. This would account for the relative stability of this enzyme.

Since the implication from the kinetic studies (vide infra) is that a major conformational change takes place upon binding

A

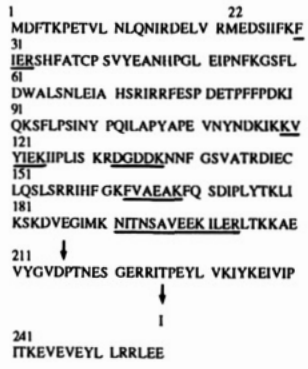

B

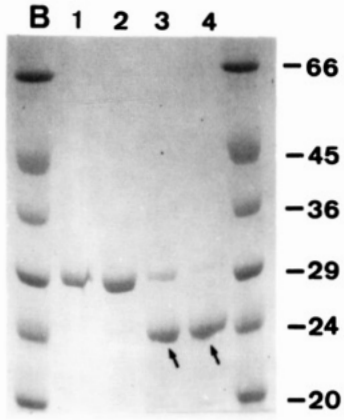

C

amino acid	residues per molecule found	predicted
Asx	25.9	27
Glx	28.9	30
Ser	16.1	17
Gly	9.5	8
His	4.0	4
Arg	14.8	15
Thr	11.0	11
Ala	11.0	11
Pro	13.8	16
Tyr	9.5	10
Val	14.1	15
Met	1.5	3
Ile	23.6	27
Leu	20.2	20
Phe	11.0	14
Lys	28.7	23

FIGURE 2: Amino acid analysis and formate cleavage of the wild-type chorismate mutase. (A) Peptide sequence of the chorismate mutase deduced from the *ARO7* DNA sequence. The amino acid sequence of the underlined tryptic fragments was determined and corresponds to the amino acid sequence deduced from the *ARO7* DNA sequence. Arrows indicate the formate cleavage site at positions 215/216 and the amino acid substitution Thr to Ile of the mutant enzyme at position 226. (B) 15% SDS–polyacrylamide gel of wild-type chorismate mutase cleaved by formate. (1) 4 μg of chorismate mutase. Samples 2–4 were incubated at 37 °C as the following: (2) 48 h in 50 mM potassium phosphate buffer as control without formate; (3) 48 h in 70% formate; (4) 72 h in 70% formate. The arrows indicate the cleaved peptide fragment with a molecular weight of approximately 25 000. The size markers are indicated on the right in kilodaltons and are the same as those used in Figure 1. (C) Amino acid composition of the wild-type chorismate mutase. The predicted values are based on the amino acid sequence deduced from the DNA sequence (Schmidheini et al., 1989). No values are given for cysteine and tryptophan.

of tryptophan, it is desirable to characterize this in structural terms. The inordinate line widths of the ^{1}H NMR spectrum of chorismate mutase result in negligible differences without and with tryptophan (data not shown). However, there are differences in the ^{13}C NMR spectra of the enzyme upon addition of tryptophan, and this is under further investigation.

Substrate Kinetics. Kinetic analyses with the pure enzyme of both the wild-type and the mutant chorismate mutase were performed to determine the steady-state kinetic parameters. A sigmoidal substrate saturation was found for the wild-type enzyme in the absence of either the inhibitor tyrosine or the activator tryptophan (Figure 4A). V_{max}, the Hill coefficient n, and $[S]_{0.5}$ were determined by using the Marquardt procedure (Marquardt, 1963) and the Hill equation $v/V_{max} = [S]^n/(K' + [S]^n)$, which is a simplified velocity equation for allosteric enzymes (Segel, 1975). This strong positive cooperativity, with an $[S]_{0.5}$ of 4 mM and a Hill coefficient n = 1.71, was increased in the presence of 300 μM tyrosine as inhibitor: $[S]_{0.5}$ = 8.6 mM and n = 1.86 (Table I). The cooperativity was abolished in the presence of 10 μM tryptophan, with a reduced $[S]_{0.5}$ of 1.2 mM and a Hill coefficient of n = 1.00, giving a normal Michaelis–Menten substrate saturation curve (Figure 4A). Similar Hill coefficient values were calculated by using the $[S]_{0.9}/[S]_{0.1} = 81^{1/n}$ equation (data not shown). The n values in the presence of tyrosine or in the absence of amino acids clearly exceed 1.0, indicating that the chorismate mutase binds at least two substrate molecules. Both $[S]_{0.5}$ and also the maximal velocity V_{max} are altered by tyrosine inhibition, which is typical for mixed inhibition.

Surprisingly, normal Michaelis–Menten substrate saturation was found for the mutant enzyme, with similar parameters as the wild-type enzyme measured in the activated state (Figure 4B; Table I). The same curve was observed in the presence of tryptophan or tyrosine, reflecting the unresponsive character of the enzyme carrying a single amino acid substitution. With the V_{max} values and the known enzyme amount e_0, the turnover numbers $[k_{cat} = V_{max}/(e_0/M_r)]$ could be calculated for the wild type and the mutant enzyme (Table I).

Action of Inhibitor and Activator on the Wild-Type Chorismate Mutase. The action of inhibitor and activator was investigated only for the wild-type enzyme because the mutant enzyme showed no response toward tyrosine and tryptophan. The type of inhibition suggested by substrate saturation experiments (mixed inhibition) was further investigated by plotting $[S]/v$ versus inhibitor concentration, [I]. In the presence of 1–4 mM substrate concentrations, all lines drawn by the linear least-squares fit method cross in one point representing a K_i of 50 μM (Figure 5). This agrees with the model of mixed inhibition, where this set of lines intersect at one point in contrast to the competitive inhibition (Cornish-Bowden, 1976).

The interplay of activator and inhibitor was characterized by the method of Whitehead (1970). Interpreting the wild-type chorismate mutase as a T–R system according to the common model for allosteric enzymes, the addition of the inhibitor tyrosine (I) will pull the protein toward the T state, and the addition of the activator tryptophan (A) will pull the protein toward the R state. Simultaneous addition of inhibitor and activator will give rise to linear and convergent isoactivity plots of [A] versus [I]. Points on these lines exhibit the same T–R equilibrium and, hence, the same initial velocity. For the wild-type chorismate mutase, a set of different lines representing initial velocities ranging from 5 to 30 milliunits

Table I: Steady-State Kinetics of the Wild-Type and the Mutant Chorismate Mutase[a]

	$[S]_{0.5}$ (mM)			Hill coefficient, n			k_{cat} (s^{-1})		
	−amino acid	+Tyr	+Trp	−amino acid	+Tyr	+Trp	−amino acid	+Tyr	+Trp
wild type	4.0	8.6	1.2	1.71	1.86	1.00	176	129	264
mutant	1.0			1.07			219		

[a] +Tyr, tyrosine was added to a final concentration of 300 μM. +Trp, tryptophan was added to a final concentration of 10 μM.

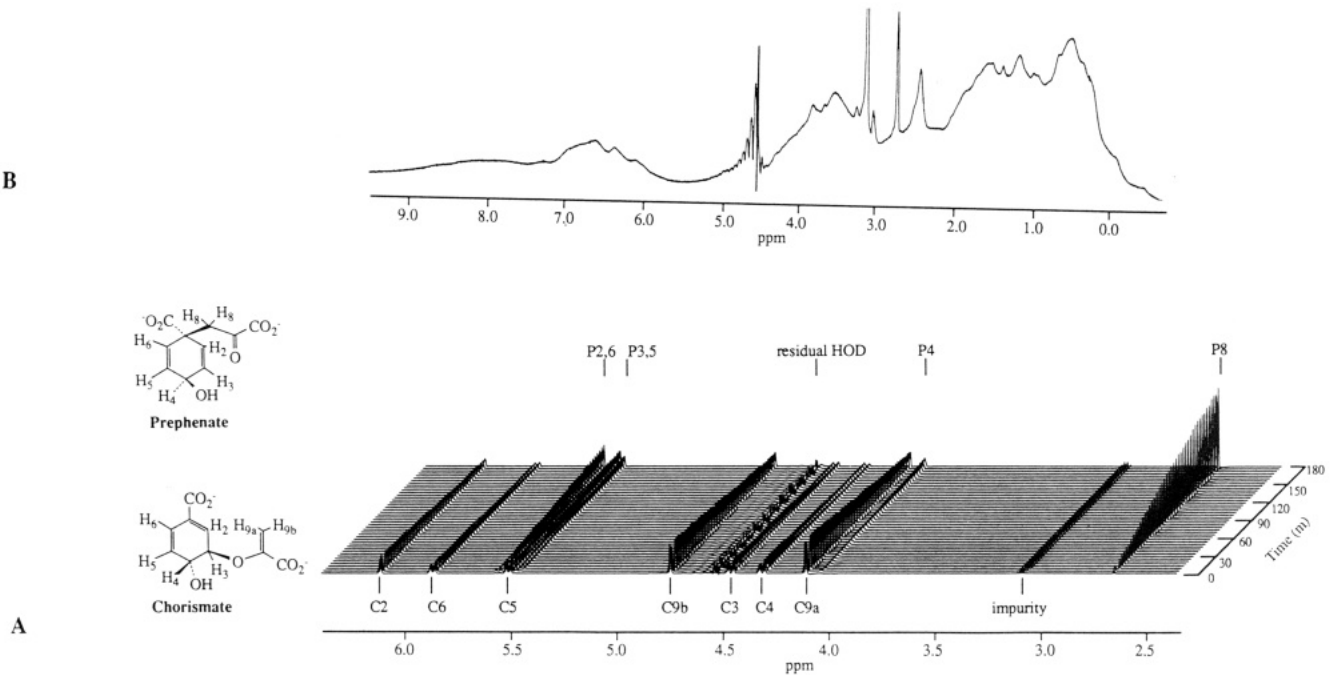

FIGURE 3: 500-MHz ^1H NMR spectra of (A) chorismate (10 mM) plus chorismate mutase (50 μM) in 50 mM potassium phosphate in 99% (v/v) D_2O/H_2O, pH 7.6, total volume = 450 μL [assignments for chorismate (C) and the product prephenate (P) are marked on the appropriate resonances], and (B) chorismate mutase (2 mM) in 10 mM potassium phosphate, pH 7.6. The sharp resonances at 2.8 and 3.2 ppm are due to residual glycerol. All spectra were obtained at 4 °C, with number of scans = 288 (A) or 1500 (B), recycle time = 1.2 s, pulse width = 3 μs (90°), size = 8K data points, and the FID's Fourier transformed with line broadening = 1 Hz.

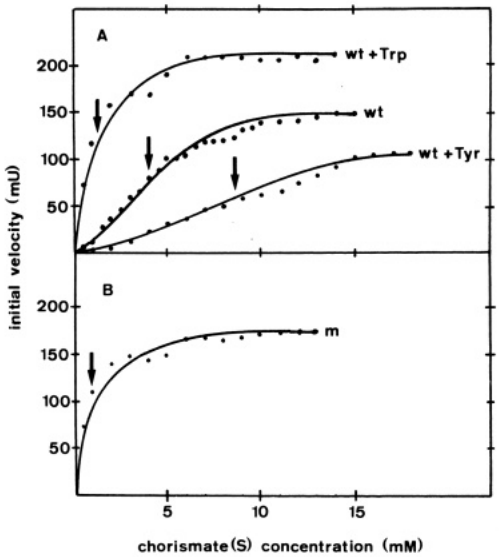

FIGURE 4: Substrate saturation for the wild-type (A) and the mutant (B) chorismate mutase. Sigmoidal curves were obtained for the wild-type enzyme in the presence of 100 μM Tyr (wt + Tyr) and in the absence of amino acid (wt). In the presence of 10 μM Trp (wt + Trp), however, the wild-type enzyme shows a hyperbolic substrate saturation curve. The same hyperbolic curve was obtained for the mutant enzyme (m), regardless of whether measured in the presence or absence of amino acid. The $[S]_{0.5}$ values are indicated by arrows, and both V_{max} and $[S]_{0.5}$ are listed in Table I. Each measurement was performed at least twice.

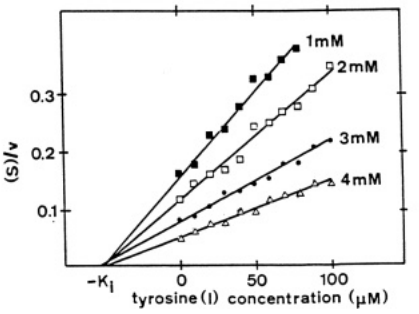

FIGURE 5: Action of inhibitor and activator on the wild-type chorismate mutase. [S] [chorismate)/v versus [I] (tyrosine) plot for the wild-type chorismate mutase. Substrate concentration was varied from 1 to 4 mM. All lines were drawn by the linear least-squares fit method. K_i is 50 μM and was determined as a median of all points of intersection. Each measurement was performed at least twice, and the standard deviation did not exceed 20%.

intersect in one point (data not shown). The K_i for tyrosine was determined as 70 μM and differs only slightly from the above value (50 μM). The K_a for tryptophan was 1.5 μM.

The dependence of initial velocity on inhibitor or activator was also investigated in two separate experiments with constant substrate concentration, plotting v versus inhibitor or activator concentration. The wild-type chorismate mutase attains half-maximal activation at a 2.5 μM tryptophan concentration, whereas half-maximal inhibition needs 40 μM tyrosine (data not shown).

pH Optima for the Chorismate Mutase. The specific enzyme activities of the wild-type enzyme in the absence of amino acids or in the presence of tyrosine or tryptophan, as well as of the mutant enzyme, were determined over a pH range of 2–10 (Figure 6). The wild-type chorismate mutase shows a

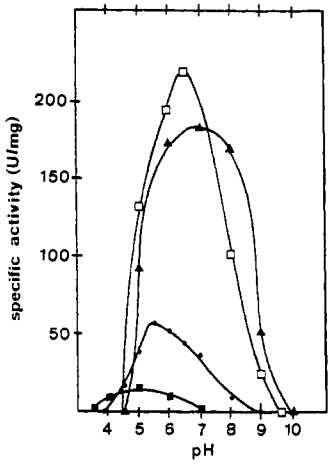

FIGURE 6: pH optima for the wild-type and mutant chorismate mutase under different incubation conditions. The wild-type enzyme was measured in the presence of 500 μM Trp [(▲); pH optimum 7.0], in the absence of amino acids [(●); pH optimum 5.5], and in the presence of 500 μM Tyr [(■); pH optimum 5.0]. The pH optimum for the mutant enzyme (□) was determined as 6.3. Each measurement was performed at least twice.

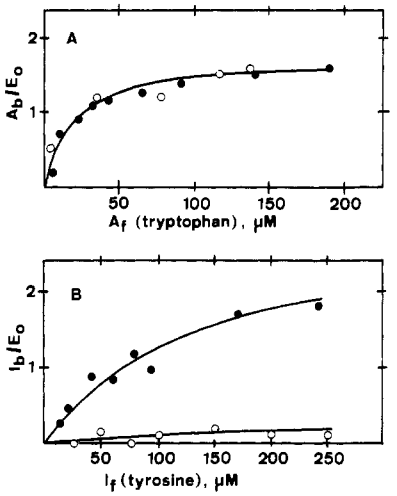

FIGURE 7: Binding plot for tryptophan (A) and tyrosine (B) to the wild-type (●) and the mutant (○) chorismate mutase obtained from equilibrium dialysis experiments. Bound (A_b) and free (A_f) tryptophan concentrations were measured and A_b/E_0 was plotted versus A_f. The same was performed for tyrosine. A 14.5 μM enzyme solution (E_0) was used. Each measurement was performed at least twice.

pH optimum at 5.5, whereas in the presence of tryptophan the highest activity is found at pH 7.0. The pH optimum is even lower in the presence of tyrosine (5.0). It is interesting that tryptophan acts only in a certain range as activator, but as an "inhibitor" at a lower pH. The single amino acid substitution in the wild-type enzyme altered the pH optimum to 6.3 for the mutant enzyme.

Binding Sites for Tryptophan and Tyrosine on the Chorismate Mutase. We determined the number of binding sites for tryptophan and tyrosine on both wild-type and mutant enzymes by using equilibrium dialysis (Englund et al., 1969). Binding of L-tryptophan and L-tyrosine at 30 °C, determined by using solutions of 14.5 μM chorismate mutase, is shown in Figure 7. Both the wild-type and also the mutant enzymes were capable of binding more than one tryptophan molecule, indicating that both enzymes have two tryptophan binding sites (Figure 7A). For tyrosine, however, only the wild-type enzyme was able to bind two molecules, whereas no binding was observed for the mutant enzyme (Figure 7B), suggesting that there are two conformational states for the wild type but only one for the mutant enzyme.

Discussion

The *S. cerevisiae ARO7* gene product chorismate mutase is a branch-point enzyme in the aromatic amino acid biosynthetic pathway and thus, together with anthranilate synthase, responsible for the distribution of chorismate. We investigated the regulation of the purified chorismate mutase and compared it with a mutant chorismate mutase which was changed by a single amino acid substitution in the C-terminal part of the protein.

Using overexpressing strains carrying the previously isolated wild-type and mutant *ARO7* allele (Schmidheini et al., 1989), we have devised a rapid method to purify the corresponding enzymes. A single Thr226 to Ile226 substitution in the mutant enzyme results in a 10-fold increased activity, obviating the need for tryptophan activation. The mutant enzyme fails to respond to tyrosine inhibition and is therefore locked in the activated state. Overexpression of this enzyme leads to starvation for tryptophan because of depletion of the chorismate pool in such a way that the other branch-point enzyme, anthranilate synthase, can no longer channel any intermediates in the direction of tryptophan biosynthesis. An 11 000-fold enrichment is necessary to obtain pure preparations of both enzymes. On this basis, chorismate mutase represents approximately 0.01% of the total cellular protein, and this figure correlates with the estimated *ARO7* mRNA level in the cell, which, based on the codon usage index according to Bennetzen and Hall (1982), amounts to roughly 0.01%. Compared to other aromatic amino acid biosynthetic enzymes, the chorismate mutase is more abundant than, e.g., the phosphoribosyl-anthranilate isomerase (0.006%; Braus et al., 1988) but less abundant than, e.g., the anthranilate synthase/indole-3-glycerol-phosphate synthase complex (0.05%; Prantl et al., 1985) or the (phenylalanine-inhibitable) DAHP-synthase (0.08%; Paravicini et al., 1989b).

As was reported for other yeast enzymes like the *TRP3* gene product indole-3-glycerol-phosphate synthase (Prantl et al., 1985) and the *TRP5* gene product tryptophan synthase (Zalkin & Yanofsky, 1982), the N-terminus was blocked, suggesting that at least some of the aromatic amino acid biosynthetic enzymes in yeast are modified at their N-terminus. However, by specific cleavage of the protein, the translational start codon of the *ARO7* gene could be determined, and the experimentally calculated amino acid composition agrees well with the deduced amino acid sequence. By sequencing peptide fragments generated by tryptic digestion, parts of the earlier DNA sequence could be confirmed.

Studies based on both gel filtration and ultracentrifugation indicated that the chorismate mutase consists of two identical subunits. The binding of tryptophan did not result in either association or dissociation of the dimers.

The reaction catalyzed by chorismate mutase was originally thought (Ife et al., 1976) to be the only example of a pericyclic reaction in primary metabolism. The enzyme from *E. coli* occurs in two forms as a bifunctional (chorismate mutase–prephenate dehydrogenase and chorismate mutase–prephenate dehydratase) dimeric protein (M_r 84 000 per dimer) with overlapping active sites (Davidson, 1987; Davidson & Hudson, 1987). This has been studied extensively in the absence of NAD^+, which is required for prephenate dehydrogenase activity, although this has complicated any attempts to study ligand binding or active-site mapping. Stereochemical studies have shown that the enzymic (Sogo et al., 1984; Asano et al., 1985) and the nonenzymic (Copley & Knowles, 1985) reaction each proceed through a transition state of chairlike geometry

(i.e., the higher energy diaxal conformation). The concertedness of both enzymic and nonenzymic rearrangements has been probed by Addadi et al. (1983) through the use of secondary isotope effects. The nonenzymic rearrangement shows a secondary tritium isotope effect at C-5 (the site of bond breaking) but none at C-9 (the site of bond formation), which suggests either a stepwise reaction or a very unsymmetrical transition state. However, no isotope effect at either site was observed for the enzyme-catalyzed rearrangement, implying that the rate-limiting transition state occurs before the rearrangement. More recently, Copley and Knowles (1987) have shown that the nonenzymic rearrangement involves a dipolar transition state having some of the character of a tight ion pair between the enolpyruvate anion and the cyclohexadienyl cation. This finding is consistent with recent evidence (Coates et al., 1987; Gajewski et al., 1987) which suggests that the acid-catalyzed Claisen rearrangement proceeds via dissociative, dipolar transition states. Consequently, Knowles and coworkers (Guilford et al., 1987) have proposed a mechanism for chorismate mutase in which a covalent enzyme–intermediate complex forms, with generation of the enolpyruvyl anion. In such a mechanism, it is conceivable that pyruvate is released into free solution. With purified monofunctional chorismate mutase available, it has been possible to examine the enzymatic reaction for the first time by ^{1}H NMR spectroscopy. The observed turnover of chorismate to prephenate without accumulation of intermediate indicates that if the mechanism of Knowles et al. is correct, no pyruvate can be detected in free solution under the conditions of our experiment.

The finding that the chorismate mutase is a dimer agrees with the result that the chorismate mutase is an allosteric enzyme with a Hill coefficient of 1.71 in the absence of amino acid, indicating that the enzyme has at least two substrate binding sites. The wild-type enzyme can be described according to the Monod–Wyman–Changeux model as a dimer in which both subunits exist in either a T state or a R state. According to that model, addition of tryptophan as an activator stabilizes the R state, which has a lower $[S]_{0.5}$ value, as was observed for the wild-type enzyme. Tyrosine has the opposite effect. Different inhibitor and activator concentrations in a constant ratio thus modulate a T–R equilibrium which is constant and which has the same initial velocity as represented in a Whitehead plot for the chorismate mutase. The possibility that tryptophan activates through a dimerization of the chorismate mutase was excluded by a gel filtration experiment. The same effect, namely, cooperativity which is destroyed in the presence of an activator leading to normal Michaelis–Menten substrate saturation, has been observed for other allosteric enzymes such as the isocitrate dehydrogenase of *S. cerevisiae* (Hathaway & Atkinson, 1963) and the deoxythymidine kinase of *E. coli* (Okazaki & Kornberg, 1964).

The finding that tyrosine lowers both $[S]_{0.5}$ and V_{max} is strong evidence for mixed inhibition. This is now the subject of further experiments, including X-ray analysis, to determine the proximity of the tyrosine, the tryptophan, and the chorismate binding sites.

The amino acid change in the mutant enzyme causes a shift in the T–R state equilibrium in favor of the R state which is not capable of binding tyrosine. This explains the drastic decrease of $[S]_{0.5}$ in the mutant enzyme which is equal to that $[S]_{0.5}$ of the R state in the wild-type enzyme. Recently a tryptophan auxotrophic mutant strain of *Pichia guilliermondii* was isolated with a 7-fold increased chorismate mutase activity, leading to a depletion of the chorismate pool (Bode et al., 1989). The cooperativity of the wild-type enzyme was lost in this mutant enzyme. Once the cloned gene and the purified enzyme will be available, it will be interesting to compare it with the *S. cerevisiae* chorismate mutases.

Compared to other aromatic amino acid biosynthetic enzymes of *S. cerevisiae*, the turnover number (k_{cat}) of the chorismate mutase, varying from 176 to 264 s^{-1}, is clearly higher than that of the phosphoribosyl-anthranilate isomerase (50 s^{-1}; Braus et al., 1988), indole-3-glycerol-phosphate synthase (2 s^{-1}; Braus et al., 1988), phosphoribosyl transferase (2.9 s^{-1}; Hommel et al., 1989), or (phenylalanine-inhibitable) DAHP-synthase (10 s^{-1}; Paravicini et al., 1989b).

The different pH optima for the wild-type enzyme measured under three different conditions (in the absence of amino acids, in the presence of tryptophan, and in the presence of tyrosine) and for the mutant enzyme can also be explained by using the Monod–Wyman–Changeux model. This suggests that there are two states with different conformations for the wild-type enzyme. Each state has a different pH optimum: the T state of the enzyme has a pH optimum at 5.0 and the R state at pH 7.0. In the absence of amino acids, the enzyme exists in a T–R equilibrium and has a pH optimum between 5.0 and 7.0. The R state (modulated by tryptophan) has almost no activity at pH 5.0, which clarifies the result that tryptophan acts as an "inhibitor" at low pH. The mutant enzyme mainly exists in the R state and thus has an optimum which is shifted toward 7.0.

Point mutations are one basis for evolution. The two described yeast chorismate mutases thus demonstrate the striking effect of a point mutation within a gene on the function of its gene product. Using NMR and X-ray analysis, the two enzymes may represent an ideal model for studying the R state of an allosteric enzyme in comparison to the T–R equilibrium.

Acknowledgments

We thank Prof. R. Hütter for generous support and Prof. K. Kirschner for advice on equilibrium dialysis. Ariel Lustig determined the native molecular weight on an ultracentrifuge. We thank Tony Willis for the amino acid sequence determination, Paul Barlow for help in purification of the chorismate mutase, Marc Eberhardt for the computer analysis of the kinetic data, and G. Paravicini and S. Irniger for helpful discussions. Our thanks are due to David Jones for critical reading of the manuscript.

Registry No. Thr226, 72-19-5; Ile226, 73-32-5; chorismate mutase, 9068-30-8; tryptophan, 73-22-3; tyrosine, 60-18-4.

References

Addadi, L., Jaffe, E. K., & Knowles, J. R. (1983) *Biochemistry 22*, 4494–4501.

Aebersold, R. H., Laevitt, J., Saavedraa, R. A., Leroy, E. H., & Kent, S. B. H. (1987) *Proc. Natl. Acad. Sci. U.S.A. 84*, 6970–6974.

Asano, Y., Lee, J. J., Shieh, T. L., Spreafico, F., Kowal, C., & Floss, H. G. (1985) *J. Am. Chem. Soc. 107*, 4314–4320.

Beggs, J. D. (1978) *Nature (London) 275*, 104–109.

Bennetzen, J. L., & Hall, B. D. (1982) *J. Biol. Chem. 257*, 3026–3031.

Bode, R., Koll, P., Prahl, N., & Birnbaum, D. (1989) *Arch. Microbiol. 151*, 123–125.

Bradford, M. M. (1976) *Anal. Biochem. 72*, 248–254.

Braus, G., Luger, K., Paravicini, G., Schmidheini, T., Kirschner, K., & Hütter, R. (1988) *J. Biol. Chem. 263*, 7868–7575.

Coates, R. M., Rogers, B. D., Hobbs, S. J., Peck, D. R., & Curran, D. P. (1987) *J. Am. Chem. Soc. 109*, 1160–1170.

Copley, S. D., & Knowles, J. R. (1985) *J. Am. Chem. Soc. 107*, 5306.
Copley, S. D., & Knowles, J. R. (1987) *J. Am. Chem. Soc. 109*, 5008-5013.
Cornish-Bowden, A. (1976) in *Principles of Enzyme Kinetics*, pp 57-61, Butterworth Press, London.
Davidson, B. E. (1987) *Methods Enzymol. 142*, 432-439.
Davidson, B. E., & Hudson, G. S. (1987) *Methods Enzymol. 142*, 440-450.
Dawson, R. M. C., Elliot, D. C., Elliot, W. H., & Jones, K. M. (1969) in *Data for Biochemical Research*, 2nd ed., p 485, Clarendon Press, Oxford.
Englund, P. T., Huberman, J. A., Jovin, T. M., & Kornberg, A. (1969) *J. Biol. Chem. 244*, 3038-3044.
Gajewski, J. J., Jurayj, J., Kimbrough, D. R., Gande, M. E., Ganem, B., & Carpenter, B. K. (1987) *J. Am. Chem. Soc. 109*, 1170-1186.
Guilford, W. J., Copley, S. D., & Knowles, J. R. (1987) *J. Am. Chem. Soc. 109*, 5013-5019.
Hathaway, J. A., & Atkinson, D. E. (1963) *J. Biol. Chem. 238*, 2875-2881.
Hinnebusch, A. G. (1988) *Microbiol. Rev. 52*, 248-273.
Hommel, U., Lustig, A., & Kirschner, K. (1989) *Eur. J. Biochem. 180*, 33-40.
Ife, R. J., Ball, L. F., Lowe, P., & Haslam, E. (1976) *J. Chem. Soc., Perkin Trans. 1*, 1776-1783.
Jenissen, H. P., & Heilmeyer, L. M. G. (1975) *Biochemistry 14*, 754-760.
Kradolfer, P., Zeyer, J., Miozzari, G., & Hütter, R. (1977) *FEMS Microbiol. Lett. 2*, 211-216.
Landon, M. (1977) *Methods Enzymol. 47*, 145-149.
Lowry, O. H., Rosebrough, N. J., Farr, A. L., & Randall, R. J. (1951) *J. Biol. Chem. 193*, 265-275.
Marquardt, D. W. (1963) *J. Soc. Ind. Appl. Math. 11*, 431-456.
Miozzari, G., Niederberger, P., & Hütter, R. (1978) *J. Bacteriol. 134*, 48-59.
Monod, J., Wyman, J., & Changeux, J.-P. (1965) *J. Mol. Biol. 12*, 88-118.
Okazaki, R., & Kornberg, A. (1964) *J. Biol. Chem. 239*, 275-284.
Paravicini, G., Mösch, H. U., Schmidheini, T., & Braus, G. (1989a) *Mol. Cell. Biol. 9*, 144-151.
Paravicini, G., Schmidheini, T., & Braus, G. (1989b) *Eur. J. Biochem. 186*, 361-366.
Prantl, F., Strasser, A., Aebi, M., Furter, R., Niederberger, P., Kirschner, K., & Hütter, R. (1985) *Eur. J. Biochem. 146*, 95-100.
Schmidheini, T., Sperisen, P., Paravicini, G., Hütter, R., & Braus, G. (1989) *J. Bacteriol. 171*, 1245-1253.
Segel, I. H. (1975) in *Enzyme Kinetic*, pp 346-464, Wiley, New York.
Sogo, S. G., Widlanski, T. S., Hoare, J. H., Grimshaw, C. E., Berchtold, G. A., & Knowles, J. R. (1984) *J. Am. Chem. Soc. 106*, 2701-2703.
Whitehead, E. P. (1970) *Prog. Biophys. Mol. Biol. 21*, 321.
Zalkin, H., & Yanofsky, C. (1982) *J. Biol. Chem. 257*, 1491-1500.

Glucosamine-6-phosphate Synthase from *Escherichia coli*: Determination of the Mechanism of Inactivation by N^3-Fumaroyl-L-2,3-diaminopropionic Derivatives†

Nathalie Kucharczyk, Marie-Ange Denisot, François Le Goffic, and Bernard Badet*
Laboratoire de Bioorganique et Biotechnologies, UA CNRS 1389, ENSCP, 11 rue Pierre et Marie Curie, 75231 Paris Cedex 05, France

Received September 28, 1989; Revised Manuscript Received December 14, 1989

ABSTRACT: A mechanistic investigation of the inactivation of *Escherichia coli* glucosamine-6-phosphate synthase by N^3-(4-methoxyfumaroyl)-L-2,3-diaminopropionate (FMDP) was undertaken. On the basis of the known participation of the *N*-terminal cysteine residue in this process [Chmara et al. (1986) *Biochim. Biophys. Acta 870*, 357; Badet et al. (1988) *Biochemistry 27*, 2282], the model reactions between FMDP and L-cysteine and between FMDP and the synthetic decapeptide Cys-Gly-Ile-Val-Gly-Ala-Ile-Ala-Gln-Arg, corresponding to the amino-terminal protein sequence, were studied. The results allowed us to propose a pathway that is in perfect agreement with the biochemical results: enzyme inactivation arose from Michael addition of glutamine binding site cysteine-1 on the fumaroyl double bond at the β-position of the ester group. Upon denaturation under slightly alkaline conditions, this adduct underwent cyclization to a transient succinimide adduct, which rearranged into the stable 2-substituted 1,4-thiazin-3-one-5-carboxylate involving participation of the cysteine amino group. The tryptic radiolabeled peptides purified from [^{3}H]FMDP-treated enzyme and resistant to Edman degradation coeluted with the products resulting from the model reaction between the synthetic decapeptide and the inhibitor.

Of all microbial infections in humans, the mycoses, particularly those affecting immunocompromised patients, are the most difficult to cure. Although real progress has been made in the development of antifungal drugs (Drouhet et al., 1987; Stevens, 1987; Graybill, 1989), only a few are active both in vitro and in vivo. The problems at present include the need for more effective agents, particularly with a novel mode of action. Glucosamine-6-phosphate synthase has been recognized only quite recently (Kenig et al., 1976; Chmara et al., 1984; Andruszkiewicz et al., 1984; Milewski et al., 1988) as a potential target for antibacterial and antifungal drug design.

† Financial support from Agence Nationale pour la Valorisation de la Recherche (N.K.) and from Ligue Nationale Contre Le Cancer (M.-A.D.).
* To whom correspondence should be addressed.

0006-2960/90/0429-3668$02.50/0